



33 This energy is then converted to electrical energy in a generator. Due to the need of a 20 °C
34 difference between the cold deep and the warm surface waters for the OTEC exploitation, tropical
35 areas are well suited for the installation of OTEC plants.

36 The Martinique, a tropical island of Lesser Antilles, is ideally suited for OTEC functioning with its
37 narrow continental slope in the Caribbean part of the island, allowing an implementation of the plant
38 close to the coast. The implementation of a 10 MW OTEC pilot plant off the Caribbean coast of
39 Martinique is expected in 2020 as part of the french NEMO project (Akvo Energy, DCNS). This
40 OTEC will pump approximately 100 000 m³.h⁻¹ of deep seawater at 1100 m depth. In order to
41 optimize the energy efficiency, the deep seawater should be rejected close to the surface. However,
42 this large discharge could induce important disturbances on the upper ocean ecosystem, and this
43 impact should be estimated.

44 Environmental assessment of OTEC functioning was studied since the 1980's (NOAA, 1981;
45 2010). The deep seawater discharge was described as one of the major drivers impacting the marine
46 environment in OTEC plant. However, only a few studies specifically detailed this critical aspect
47 (Taguchi et al., 1987; Rocheleau et al., 2012). The deep seawater discharge in OTEC plant generates
48 a phenomenon similar to the one naturally occurring in the ocean within upwelling systems.
49 Equatorward winds along the coast in the eastern Atlantic and Pacific linked to atmospheric high-
50 pressure systems force Ekman transport and pumping, relocating coastal surface waters offshore.
51 Thereby, deep water transport towards the surface is generated close to the coast. In these systems,
52 the large amount of macronutrients and trace metals carried to the euphotic zone by the enriched
53 deep seawater supports a large development of the phytoplankton, making upwelling the most
54 productive oceanic regions (Bakun, 1990; Pauly and Christensen, 1995; Chavez and Toggweiler,
55 1995; Carr and Kearns, 2003). The tropical surface waters off the Caribbean coast of Martinique
56 exhibit low nutrients concentrations and can be significantly enriched by the deep seawater
57 discharge. Whereas phytoplankton assemblages in upwelling systems are usually dominated by large
58 phytoplankton and particularly by diatoms (Bruland et al., 2001; Van Oostende et al., 2015), the
59 phytoplankton community in oligotrophic systems is composed of smaller organisms (Agawin et al.,
60 2000).

61 Due to these important differences, it is thus of critical interest to investigate the potential effects of
62 the deep seawater discharge of the planned OTEC plant on the phytoplankton community off
63 Martinique.

64 In this study, the impact of deep seawater discharge on the thermal structure of surface
65 waters was first assessed. Modification of the surface waters stratification should indeed impact the
66 phytoplankton community. It is crucial to provide a depth where the deep seawater could be



67 discharged without significant effect on the surface layer where phytoplankton is the most abundant.
68 A high-resolution oceanic model was used to examine the thermal impact induced by the deep
69 seawater dispersion. Eight configurations of discharge depth were tested, corresponding to the
70 deep chlorophyll-a maximum (DCM), the bottom of the euphotic layer (BEL) and five depths below
71 the BEL. Temperature differences between numerical simulations without and with the deep
72 seawater discharge were compared on the upper 150 m of a vertical section.

73 The distribution of the ambient phytoplankton community and the biogeochemical
74 properties of the deep and surface seawater mixture that could impact the phytoplankton
75 community were then described. Phytoplankton distribution and assemblage were detailed in order
76 to assess short time and small scales variabilities of phytoplankton assemblage and primary
77 production in the study site.

78 Finally, in order to simulate the OTEC deep seawater input, enrichment experiments were
79 conducted on the future site of the pilot plant. Enrichment experiments are commonly used in
80 oceanography to assess the effects on phytoplankton community and primary production. For
81 example, large iron (Fe) enrichment experiments were conducted from 1993 to 2005 to estimate the
82 potential of Fe limitation on ocean primary production (De Baar et al., 2005; Boyd et al., 2007).
83 Several experiments also showed that macro- and micro-nutrients enrichments induce changes in the
84 phytoplankton community in upwelling regions (Hutchins et al., 2002) as well as in oligotrophic
85 regions (Kress et al., 2005). Enrichment experiments were usually conducted with mesocosms
86 immersed close to the surface (Escaravage et al., 1996; Duarte et al., 2000) or in laboratory under
87 artificial light and temperature using phytoplankton model species (Brzezinski, 1985). A laboratory
88 experiment intended to evaluate the effects of an OTEC seawater discharge in Hawaiian waters on
89 the natural phytoplankton community was previously conducted (Taguchi et al., 1987) under such
90 artificial conditions, and thus, it could not totally reproduce what occurred in the natural
91 environment. Other deep seawater discharge experiments were realized *in situ* (Aure et al., 2007;
92 Handå et al., 2014). For example, the use of a moored platform to upwell deep seawater and
93 discharge it close to the surface has shown an increase in primary production in a western
94 Norwegian fjord where the euphotic zone is nutrient-depleted during summer (Aure et al., 2007), as
95 it would be expected with the OTEC discharge. Whereas such a pumping system is well adapted for
96 pumping seawater at 30 m depth for example, it cannot be applied for OTEC experiments where
97 deep seawater must be collected far deeper (1100 m depth) and also discharged more deeply in the
98 water column to reduce the potential effects on the phytoplankton community. These conditions can
99 be obtained by the use of *in situ* microcosms, in which light and temperature are the same as in the
100 natural surrounding waters, avoiding additional bias, and several conditions (enrichment, incubation



101 depth) can be simulated. Therefore, we used the unique device of immersed microcosms we
102 developed (Giraud et al., 2016) for assessing the effects of deep seawater discharge on the
103 phytoplankton community. Two incubation depths (DCM and BEL) with two ratios of enriched
104 seawater (mixtures of surface water with 2 % and 10 % of deep seawater) were tested. These
105 experiments allowed the evaluation of critical mixing rate and discharging depth where effect was
106 maximal.

107

108 2. Materials and methods

109 2.1. Modelling the thermal effect

110 The hydrodynamic numerical model ROMS-Regional Ocean Model System (Shchepetkin and
111 McWilliams, 2005; 2009) was used to describe the resulting thermal effect due to OTEC functioning.
112 The model was run in a 2-ways AGRIF configuration allowing to define a parent and child domains
113 around the Martinique Island which are run simultaneously, transferring automatically open boundary
114 conditions. The parent grid ranges from 63° W to 59° W and 13° N to 15.9° N with a resolution of
115 1/60° (around 1.8 km) while the child domain narrows the parent one and was from 61.74° W to
116 60.41° W and 14.21° N to 15.11° N with a resolution down to 1/180° (around 600 m). The bottom
117 topography and coastline are interpolated from the GINA database (1/120°,
118 www.gina.alaska.edu/data/gtopo-dem-bathymetry) (Fig. 1).

119 The model is forced by the monthly Climate Forecast System Reanalysis (NCEP-CFSR) for wind
120 stress, heat and freshwater fluxes. For the open boundary conditions and initial conditions of the
121 parent domain, a monthly climatology computed from the Simple Ocean Data Assimilation (SODA)
122 reanalysis (Carton and Giese, 2008) was used for the dynamical variables (temperature, salinity and
123 velocity fields). The NCEP-CFSR products do not cover the period of our mesocosm experiments
124 (November 2013 and June 2014). The simulations were thus performed over another period when
125 the atmospheric forcing was available. We choose the 3 years period of 1998-2000, using 1998 and
126 1999 as a spin-up and the last year 2000 to analyze the thermal structure and circulation field. Model
127 outputs were stored as daily averages. The configurations were run without and with a deep
128 seawater discharge mimicking the OTEC functioning. The deep seawater discharge was initiated on
129 January 1st 2000. Eight cases of horizontal discharge settings were simulated at different depths: 1)
130 the DCM (45 m), 2) the BEL (80 m), that were estimated on June 12th 2014, and 3) six depths below
131 the euphotic zone (110 m, 140 m, 170 m, 250 m, 350 m and 500 m). In the OTEC plant, deep water
132 will be pumped at 1100 m where temperature is around 5 °C and salinity 35. Circulation of this water
133 through the plant system will warm it up until 8 °C prior to its release in the upper ocean. We thus



134 applied at the location of the OTEC plant (61°13'0" W, 14°35'48" N), a cold water discharge
135 (temperature 8 °C, salinity 35) at a flow rate of 28 m³ s⁻¹ and with a northward orientation. The
136 thermal impact of the cold-water source was assessed documenting the differences between
137 simulations without and with the modelled OTEC plant functioning over the full year 2000.

138 2.2. Field observations and *in situ* experiments

139 2.2.1. Sampling and analytical methods

140 Temperature, salinity, and fluorescence profiles were performed using Seabird SBE19+ probe
141 with *in situ* Fluorimeter Chelsea AQUAtracka III.

142 Seawater was collected in the water column in ultra-clean conditions (Giraud et al., 2016) to
143 measure *in situ* parameters and to prepare the microcosms. Seawater and microcosms were sampled
144 similarly in a land laboratory a few hours after collection.

145 Nitrate (NO₃⁻), nitrite (NO₂⁻), phosphate (PO₄³⁻) and silicate (Si(OH)₄) concentrations were
146 determined in filtered waters (<0.6 μm PC membrane) stored at -20 °C until analysis using a Bran +
147 Luebbe AAIII auto-analyzer (Aminot and Kérouel, 2007).

148 Filtered samples (0.2 μm; 300AC-Sartobran™ capsules) for dissolved trace metals
149 determination were collected under pure-N₂ pressure (0.7 atm) in acid cleaned low density
150 polyethylene bottles, acidified with ultrapure HCl (pH < 2) and stored in two plastic bags in dark at
151 ambient temperature. Concentrations of dissolved trace metals (cadmium, Cd; lead, Pb; iron, Fe;
152 zinc, Zn; manganese, Mn; cobalt, Co; nickel, Ni; and copper, Cu) were determined in UV-digested
153 samples by ID-ICP-MS (Milne et al., 2010) after preconcentration on a WAKO resin (Kagaya et al.,
154 2009) using an Element XR ICP-MS. Blanks, limits of detection, accuracy and precision (assessed
155 using reference samples) of the ID-ICP-MS method are reported in Table 1. The values determined
156 by ID-ICP-MS were in excellent agreement with the consensus values, apart for Cd that yielded
157 higher concentration in S-SAFE reference sample than the consensus value (Table 1).

158 The pH was determined using a pH ultra-electrode (pHC28) mounted on a HQ40d multi pH-
159 meter (HACH) with an accuracy of ± 0.002 pH unit in samples preserved with saturated HgCl₂ in
160 glass bottles hermetically closed with Apiezon grease, sealed with Parafilm® and stored in the dark
161 at ambient temperature.

162 Three complementary methods were used to analyze the phytoplankton community. Pigment
163 signatures were measured by HPLC (using an Agilent Technologies 1100-series) on polysulfone
164 filters (0.22 μm pore-size) frozen at -20 °C and stored in liquid nitrogen, after internal standard
165 addition (vitamin E acetate) and extraction in a 100 % methanol solution (Hooker et al., 2012). Fifty
166 pigments were identified and associated to phytoplankton groups (Uitz et al., 2010). Identification



167 and enumeration of pico-phytoplankton were realized by flow-cytometry using a BD-FACSVerse™
168 (Marie et al., 1999) in samples preserved in cryotube with addition of 0.25 % glutaraldehyde frozen at
169 -20 °C and stored in liquid nitrogen. Four groups of pico-phytoplankton were identified:
170 *Prochlorococcus*, picoeukaryotes (< 10 µm), and 2 groups of *Synechococcus* discriminated,
171 respectively, by their low and high phycoerythrin (PUB) to phycoerythrobilin (PEB) ratios. Taxonomic
172 identification and enumeration of micro-phytoplankton (20-200 µm) and a part of nano-
173 phytoplankton (2-20 µm) (Dussart, 1966) were carried out using an inverted microscope (Wild M40)
174 in samples preserved with neutral lugol solution. Utermöhl settling chambers (Hasle, 1988) were used
175 for micro-phytoplankton analyses, and a smaller sedimentation chamber (2.97 mL) for the analyses of
176 nano-phytoplankton. When possible, phytoplankton was identified to the lowest possible taxonomic
177 level (species, genus or group). Biovolume of each species was also estimated from these
178 microscope analyses (Hillebrand et al., 1999).

179 **2.2.2. *In situ* microcosm experiments**

180 The potential impact of deep seawater discharge on the phytoplankton community was simulated
181 by *in situ* microcosm incubations of various deep and surface seawater mixing (Giraud et al., 2016).
182 The experiments were conducted from 12th (D0) to 19th (D7) of June 2014. The deep and surface
183 seawaters were collected at the site of the future OTEC pilot plant (61°11'52" W-14°37'57" N; Fig.
184 1). Microcosms bottles were incubated on two stainless steel structures set at the depths of deep
185 chlorophyll-a maximum (DCM) and at the bottom of the euphotic layer (BEL) on a mooring chain
186 located, for practical reasons, closer to the coast (61°10'9" W-14°39'8" N, seafloor at 220 m depth)
187 during 6 days (Giraud et al., 2016).

188 Seawater was collected at D0 at the depths of DCM (45 m depth) and BEL (80 m depth)
189 identified on the future OTEC site from the fluorescence profile, and close to the bottom (1100 m
190 depth corresponding to the pumping depth of the future OTEC plant) in ultra-clean conditions.
191 Deep seawater was mixed in three proportions (0 % as a control hereafter referred to as "Control", 2
192 % as a low input called "2 % of deep seawater", and 10 % as a large input called "10 % of deep
193 seawater") with DCM and BEL waters. Each resulting mixture was distributed in 2.3 L polycarbonate
194 bottles filled up to overflow level, of which four replicates per mixing condition per depth were
195 immersed at their respective sampling-depth for 6 days; duplicates per mixing condition per depth
196 were kept in dark at 25 °C for a few hours until sampling for later characterization of phytoplankton
197 assemblage and biogeochemical properties at D0 (called "Surrounding waters D0"); and duplicates
198 per mixing condition per depth were used to estimate carbon and NO₃⁻ uptakes at D0 (called
199 "Surrounding waters D0") as described below.



200 Same sampling and mixtures were realized at day 6 (D6, June 18th) just to evaluate the temporal
201 evolution in the natural environment, resting on duplicate bottles per mixing condition per depth for
202 phytoplankton and biogeochemical characterizations at D6 (called “Surrounding waters D6”) and
203 using other duplicates to estimate carbon and NO₃⁻ uptakes at D6 (called “Surrounding waters D6”).

204 After the 6 days incubation, all the incubated microcosm bottles on the mooring (called
205 “Microcosm D6”) were brought on board. A quarter of each four replicates per condition was put in
206 a new 2.3 L clean bottle and used to estimate carbon and NO₃⁻ uptakes after 6 days of incubation
207 (called “Microcosm D6”). The remaining microcosm contents were kept for sampling and analysis.

208 2.2.3. Carbon and nitrate uptakes

209 Carbon (primary production) and NO₃⁻ uptake rates were estimated in the same sample using the
210 dual ¹³C/¹⁵N isotopic label technique (Slawyk et al., 1977). Immediately after sampling, ¹³C tracer
211 (NaH¹³CO₃, 99 atom%, Eurisotop, 0.25 mmol¹³C mL⁻¹) and ¹⁵N tracer (Na¹⁵NO₃, 99 atom%, Eurisotop,
212 1 μmol¹⁵N mL⁻¹) were added to seawater mixtures at 10⁻³:1 v/v ratio. The initial enrichment was 10
213 atom% excess of ¹³C for the bicarbonate pool and 16-95 atom% excess of ¹⁵N for the NO₃⁻ pool
214 depending on the ambient NO₃⁻ concentration. The ¹³C/¹⁵N amended bottles were incubated for 24
215 h on the mooring line at the DCM and BEL depths, after which 1 L samples were filtered onto pre-
216 combusted (450 °C, 4 h) glass fiber filters (Whatman). Filters were stored at -20 °C and oven dried
217 (60 °C, 24 h) prior to analysis. Concentrations of carbon (POC), nitrogen (PON) as well as ¹³C and ¹⁵N
218 enrichments in particulate matter were measured with a mass spectrometer (Delta plus,
219 ThermoFisher Scientific) coupled to a C/N analyzer (Flash EA, ThermoFisher Scientific). Standard
220 deviations were 0.009 μM and 0.004 μM for POC and PON, and 0.0002 atom% and 0.0001 atom%
221 for ¹³C- and ¹⁵N-enrichments, respectively.

222 The absolute uptake rates (ρ , in μmol L⁻¹ h⁻¹) were calculated for nitrogen (Dugdale and Wilkerson,
223 1986) and carbon (Fernández et al., 2005) using the particulate organic concentrations measured
224 after 24 h of incubation. These rates were converted into biomass specific uptake rates (V , in μmol
225 μmol POC or PON⁻¹ h⁻¹) by dividing ρ by POC or PON. The addition of ¹⁵N tracer would cause a
226 substantial increase in dissolved inorganic nitrogen concentrations especially in the surface waters
227 and, in turn, an overestimation of uptake rates (Dugdale and Wilkerson, 1986; Harrison et al., 1996).
228 The NO₃⁻ uptake rates were corrected for this perturbation (Dugdale and Wilkerson, 1986) using a
229 half-saturation constant of 0.05 μmol.L⁻¹ characteristic for nitrogen-poor oceanic waters (Harrison et
230 al., 1996) and the measured NO₃⁻ concentration. Overestimation was low (< 5 %) in samples with an
231 addition of deep seawater but it was of about 50 % in samples without deep seawater addition. The
232 uptake rates measured in these samples represented therefore estimations rather than actual values.



233 **2.2.4. Statistical analyses**

234 Kruskal-Wallis test was applied on the set of pigments concentrations, pico-phytoplankton
235 abundances and macronutrients concentrations. If significant differences ($p < 0.05$) were found,
236 Mann-Whitney test was run to identify the samples significantly different. Statistical analyses were
237 performed using Statgraphics Centurion XVI software.

238 **3. Results**

239 **3.1. Modeling of the deep seawater discharge**

240 **3.1.1. Model evaluation**

241 We compared modeled daily profiles (temperature, salinity) of June and November 2000 with *in*
242 *situ* CTD data at OTEC station we recorded in June 2014 and November 2013 (Fig. 2 a-b).

243 In June, the modeled and observed vertical profiles of temperature were quite in agreement with
244 a well mimicked thermocline depth. However, a warm bias of ~ 1.5 °C was simulated by the model in
245 the top 50 m. Between 300 and 500 m depth, a cold bias of ~ 1.5 °C depth was also observed. The
246 modeled and experimental salinity profiles presented a similar pattern. However, the salinity was
247 largely overestimated by the model in the top-120 m, especially in the upper 60 m (by ~ 2 units), as
248 compared to field observations. Between 120 m and 150 m, the model slightly underestimated the
249 salinity.

250 In November, the thermocline and halocline were well reproduced with modeled vertical profiles
251 of temperature and salinity, in good agreement with observations. However, temperature was
252 slightly overestimated by the model, with warm bias of ~ 0.8 °C. At deeper depths, the modeled and
253 observed temperatures were in excellent agreement. Salinity was underestimated by the model
254 within the top 50 m by ~ 1 unit, and between 70 and 200 m depths by at maximum 0.3 units. Below
255 200 m depth, modeled and observed salinities exhibited similar profiles.

256 ADCP measurements (horizontal velocity and direction of currents) were made by our DCNS
257 partner at the study site for a feasibility study, but in June 2011 (between 40 m and 800 m depths).
258 ADCP data were compared to model outputs for June 2000 (Fig. 3). Current directions were quite
259 similar between model outputs and ADCP data with a mean direction toward the South/South-East.
260 The horizontal velocity norm was also quite close between both data sets with larger velocity close
261 to the surface at ~ 50 m depth. Larger difference appeared in subsurface in ADCP data but similar
262 trends were observed and values were relatively close.

263 Modeled physical properties (temperature, salinity, currents) were therefore quite similar to those
264 directly observed at the study site. The small differences observed between model and field data are



265 likely due to inter-annual variability since years examined were indeed different for the model
266 simulation (2000) and the field data (2011, 2013 and 2014).

267 **3.1.2. Impact of the deep seawater discharge on the thermal structure in surface**

268 In order to assess the deep seawater discharge impact on the thermal structure of the upper 150
269 m of the water column, the dispersion of temperature differences (ΔT in °C) obtained without and
270 with the deep seawater discharge in the model outputs was examined on two vertical sections. A
271 section of 124 km for the large domain (corresponding to the child domain) and another section of
272 10 km for the near-OTEC domain (defined from 61.24° W to 61.17° W and 14.60° N to 14.67° N)
273 were defined, both centered on the OTEC site and parallel to the coast (Fig. 1). Presently, there are
274 no environmental standards defining threshold levels for temperature difference that will be induced
275 by an OTEC deep seawater discharge. So, the study relied on the World Bank Group prescriptions
276 for liquefied natural gas facilities which set at 3 °C the temperature difference limit at the edges of
277 the zone where initial mixing and dilution take place (IFC, 2007).

278 We thus considered for each discharge depth the cooling and warming outputs from the model,
279 which exhibit a $|\Delta T| \geq 3$ °C. Areas (in % of the considered domain) impacted by these cooling and
280 warming effects were added (absolute values) in order to compare the potential impact of each
281 discharge depth configuration. None of the discharge depth configurations could produce a
282 modification of the thermal structure of the top 150 m of the water column, higher than or equal to
283 the considered temperature threshold ($|\Delta T| \geq 3$ °C), for both domains sections.

284 Then, a lower temperature difference of 0.3 °C (absolute value) was considered. This temperature
285 difference represented a low threshold as compared to the World Bank Group prescriptions (IFC,
286 2007) that instead represent a high threshold. The areas exhibiting a $|\Delta T| \geq 0.3$ °C in the top 150 m
287 (Table 2) were extremely small (< 1 km²) and were not significantly different in both sections and at
288 the different discharge depths, on an annual average and in June (our experimental period).

289 **3.2. Biogeochemical properties and phytoplankton community**

290 **3.2.1. Expected biogeochemical properties of the resulting mixed waters**

291 The pH was very similar at the DCM and BEL at the OTEC site on D6 (8.24 and 8.25,
292 respectively), whereas deep seawater-pH showed lower value (7.81). The addition of 2 % and 10 %
293 deep seawater to surface waters could thus induce a pH-decrease of respectively, 0.01 and 0.07 unit.
294 Hence, the effect on pH could be rather limited compared to the 0.1 pH decrease (from 8.2 to 8.1)
295 between the pre-industrial time and the 1990's [39].



296 NO_3^- and PO_4^{3-} concentrations (Table 3) were below the detection limit ($< 0.02 \mu\text{M}$) at the DCM
297 (55 m) and BEL (80 m) at the OTEC site on observational D4 (June 16th 2014), whereas $\text{Si}(\text{OH})_4$
298 concentrations were above detection limit ($> 0.08 \mu\text{M}$), particularly at the DCM ($2.4 \mu\text{M}$). NO_2^-
299 concentrations showed the highest values at the BEL whereas they were negligible at the DCM
300 ($< 0.02 \mu\text{M}$). In deep seawater, as commonly observed, NO_3^- , PO_4^{3-} and $\text{Si}(\text{OH})_4$ concentrations were
301 largely higher compared to the surface (Table 3). The 2 % and 10 % deep water additions
302 represented a large input for NO_3^- (from $< 0.02 \mu\text{M}$ to 0.54 and $2.71 \mu\text{M}$, respectively). If the 10 %
303 ratio also induced a large input of PO_4^{3-} (from < 0.02 to $0.19 \mu\text{M}$), the input of 2 % deep water was
304 more limited ($0.04 \mu\text{M}$). The effect of 2 % or 10 % deep seawater addition was more limited for
305 $\text{Si}(\text{OH})_4$ relatively to NO_3^- and PO_4^{3-} input, yet it accounted for 50-63 % increase for 10 % deep
306 seawater addition (Table 3). Finally, because deep and DCM waters were NO_2^- depleted, the deep
307 seawater input did not modify the NO_2^- concentration at the DCM. At the BEL, NO_2^- concentration
308 was higher and the 10 % addition slightly diluted NO_2^- at this depth.

309 Mn showed maximum concentrations in the surface layer on D4 at the OTEC site (Table 4)
310 decreasing with depth as observed close to the Lesser Antilles in the Atlantic Ocean (Mawji et al.,
311 2015), but the measured surface concentrations were particularly high, especially at the DCM. Fe
312 that commonly dispatches hybrid distribution combining a nutrient-type profile in surface waters and
313 a scavenged-type distribution in deep waters (Bruland, 2003) also exhibited high surface values,
314 particularly at the DCM (Table 4). Cd, Zn, Co, Ni, and Cu dispatched nutrient-type profiles, whereas
315 Pb exhibited scavenged-type profile (Nozaki, 1997; Gruber, 2008), but like for dissolved Fe and Mn,
316 their concentrations in the upper waters were particularly high (Table 4). For all trace metals at both
317 depths, the 2 % deep seawater addition will not induce significant changes in their surface
318 concentrations (Table 4). The 10 % deep seawater addition could increase Cd, Ni and Zn
319 concentrations in surface waters (Table 4), whereas it would not constitute an input of Pb, Cu, Co,
320 and Fe, and it can even dilute Mn (Table 4).

321 The surface waters can thus be enriched in macronutrients (NO_3^- , PO_4^{3-}) when submitted to a
322 deep seawater discharge (particularly with 10 % deep seawater addition) in proportion depending
323 on the depth. The same scheme can be applied in some of the dissolved trace metals (Cd, Ni, Zn)
324 when a large ratio of deep seawater (10 %) is discharged.

325 3.2.2. Phytoplankton community in the natural environment

326 A set of seven accessory pigments identified as biomarkers of specific taxa (Uitz et al., 2010;
327 Table 5) were analyzed at OTEC station at D0, D4 and D6 in surrounding surface waters (Fig. 4), as
328 well as population abundance and their biovolume using light microscopy (Fig. 5).



329 The total chlorophyll a (TChl a defined as the sum of chlorophyll a and divinyl chlorophyll a), a
330 proxy of the phytoplankton biomass, was higher at DCM than at BEL, as usually observed, by about
331 two-folds. The fucoxanthin (biomarker of diatoms) concentrations were similar at the DCM and BEL
332 on D0 (Fig. 4), like the total abundance of diatoms (Fig. 5). Fucoxanthin concentration increased by
333 D4 and then by D6 at the DCM, corresponding to increases of cumulated diatoms biovolume on D4
334 (Fig. 5) and of diatoms abundance on D6 (Fig. 5). Peridinin, a biomarker of dinoflagellates, was
335 detected at the DCM unlike at the BEL, with relatively high abundance and biovolume of
336 dinoflagellates (Fig. 5). The 19'-hexanoyloxyfucoxanthin (biomarker of haptophytes) concentration
337 (Fig. 4) and the prymnesiophytes (haptophyte) abundance and biovolume (Fig. 5) showed higher
338 values at the DCM than at the BEL only at D4.

339 At the DCM, dinoflagellates largely dominated the nano- and micro-phytoplankton assemblage
340 with the largest abundance and biovolume. Whereas prymnesiophytes showed the second highest
341 abundance, its biovolume was very low, on the contrary to diatoms that dispatched lower abundance
342 but higher biovolume (Fig. 5). At the BEL, dinoflagellates, prymnesiophytes and diatoms showed
343 similar abundance, dinoflagellates and the diatoms occupied the major part of the total biovolume.
344 Three groups of dinoflagellates were observed by light microscopy but they could not be identified
345 at species level. However, their small size and the lack of colored starch (using lugol) in the
346 cytoplasm suggested they were mixotrophic or heterotrophic population. Furthermore, the low
347 concentrations of peridinin in samples supported this assumption.

348 At both depths, light microscopy analyses suggested that the large cyanobacteria, mainly
349 *Trichodesmium sp.*, were low in abundance and biovolume. Flow cytometry identification and
350 count indicated that the small cyanobacteria *Prochlorococcus* dominated the pico-
351 phytoplankton assemblage, but they showed a significant decrease from D0 to D6 (Fig. 6). A
352 significant portion of *Synechococcus* was also observed while picoeukaryotes were poorly
353 represented. Both *Prochlorococcus* and *Synechococcus* showed higher abundance at the
354 DCM than at the BEL (by 65 % and 86 %, respectively), in line with the pigments analyses of
355 zeaxanthin (biomarker of cyanobacteria) and total chlorophyll *b* concentrations
356 (prochlorophytes).

357 3.2.3. Primary production and nitrate uptake in the natural environment

358 The phytoplankton distribution and assemblage can partly drive the intensity of primary
359 production, so the specific uptake rate of carbon (V_C ; Fig. 7) and NO_3^- ($V_{\text{NO}_3^-}$) were estimated at D0
360 and D6.



361 V_C in surrounding surface waters was relatively low at D0 (Fig. 7) indicating low primary
362 production in these poor-nutrients waters. Yet, V_C was approximately four-times higher at the DCM
363 ($2 \cdot 10^{-3} \text{ h}^{-1}$) than at the BEL ($5 \cdot 10^{-4} \text{ h}^{-1}$) at D0, but drastically decreasing on D6 at the DCM (to $\sim 6 \cdot 10^{-4}$
364 h^{-1}). $V_{\text{NO}_3^-}$ were also very low at D0 ($1 \cdot 10^{-3} \text{ h}^{-1}$ at DCM, $4 \cdot 10^{-3} \text{ h}^{-1}$ at BEL) and drastically decreased at
365 D6, below the detection limit (data not shown).

366 3.3. Impacts on the phytoplankton community of the deep seawater discharge

367 3.3.1. Changes in the phytoplankton assemblage

368 At the DCM, TChl *a* was similar in all treatments ($p < 0.05$) after 6 days of incubation in
369 microcosms (Fig. 8). Only fucoxanthin and 19'-butanoyloxyfucoxanthin showed significant ($p < 0.05$)
370 higher concentrations in 10 % enrichments as compared to controls, indicating higher abundance
371 and/or biovolume of diatoms and haptophytes. The other diagnostic pigments did not show any
372 significant difference between enriched microcosms and controls. Picoeukaryotes and
373 *Synechococcus* abundances did not show significant variations between the treatments (Fig. 9a).
374 Reversely, *Prochlorococcus* population showed higher ($p < 0.05$) abundance both in 2 % and 10 %
375 enriched microcosms as compared to controls (Fig. 9a).

376 At the BEL, after the 6 days incubation period, pigments concentrations were below the
377 detection limit indicating very low abundance of phytoplankton. Pico-phytoplankton did not show
378 significant variations between the treatments and the controls (Fig. 9b). Pico-phytoplankton were
379 clearly much less abundant at the BEL ($< 1000 \text{ cells mL}^{-1}$) than at DCM (Fig. 9b), 20-times even lower
380 than that observed in surrounding waters at this depth on D6. For comparison, total abundance at
381 the DCM was ~ 5 -times lower in incubated microcosms on D6 compared to surrounding surface
382 waters.

383 3.3.2. Changes in the primary production and nitrate uptake

384 Deep water inputs (2 % and 10 %) to surrounding waters collected at the DCM on D0 led to
385 an increase of V_C within 24 h compared to the controls (by 43 % and 48 %, respectively; Fig. 7); but
386 they had no effect on D6 despite very low value in natural waters at this depth ($6 \cdot 10^{-4} \text{ h}^{-1}$). The 6 days
387 incubated microcosms showed very low V_C in all treatments (Fig.7). At the BEL, V_C were quite similar
388 on D0 and D6 and after 6 days of incubation, without significant differences between the treatments
389 (Fig. 7). $V_{\text{NO}_3^-}$ measured in microcosms after a 6-days *in situ* incubation were below the detection
390 limit (data not shown).

391

392



393 **4. Discussion**

394 **4.1. Natural variabilities in the oligotrophic area**

395 **4.1.1. Modeling of the deep seawater discharge**

396 Salinity field data showed large seasonal variations, with low values in June 2014 (34.6 on the top
397 50 m) and much higher values in November 2013 (35.5 on the top 50 m). The model run for year
398 2000 did not fully reproduce these variations. Indeed, salinity was overestimated by the model in
399 June whereas it was underestimated in November. The observations we made at the OTEC station
400 showed that the low salinity observed in June was associated with high Si(OH)_4 concentrations. High
401 Si(OH)_4 levels in fresher seawater have been already reported in surface waters in the Caribbean Sea
402 and they were attributed to Amazon and Orinoco fresh rivers inputs (Steven and Brooks, 1972;
403 Moore et al., 1986; Muller-Karger et al., 1995; Hu et al., 2004). Fresh surface waters enriched in
404 Si(OH)_4 (Moore et al., 1986; Edmond et al., 1981) can be transported from the Amazon and Orinoco
405 rivers towards the Caribbean Sea by the North Brazil Current and the Guiana Current (Muller-Karger
406 et al., 1988, 1995; Osborne et al., 2014, 2015). It is likely that the rivers discharges and thus its inputs
407 in the Caribbean Sea were quite different between 2000 (modeled year) and 2014 (*in situ*
408 observations), thus explaining the discrepancy between modeled and observed salinities. Meso- and
409 submeso-scale features resulting from the rivers flows could also induce short-term variability in the
410 area and then could explain the observed differences.

411 **4.1.2. Biogeochemistry and phytoplankton community structure**

412 The very low PO_4^{3-} and NO_3^- concentrations recorded in the oligotrophic surrounding surface
413 waters were likely favorable to the development of small phytoplankton, especially to the
414 cyanobacteria as shown with the significant occurrence of *Prochlorococcus* in these waters, which are
415 typical of poor nutrient waters (Partensky et al., 1999). In line with the very low $V_{\text{NO}_3^-}$ measured here,
416 it has been shown that $V_{\text{NO}_3^-}$ by *Prochlorococcus* represents indeed only 5-10 % of its nitrogen
417 uptake whereas reduced nitrogen substrates (NO_2^- , ammonium, and urea) uptake accounts for more
418 than 90-95 % (Casey et al., 2007). By contrast, the development of larger phytoplankton taxa
419 (particularly diatoms), which have higher NO_3^- and PO_4^{3-} requirements for their growth, were
420 probably limited by these elements. Actually, NO_3^- and PO_4^{3-} concentrations in surrounding waters at
421 the DCM were both lower than the detection limit ($< 0.02 \mu\text{M}$ at D4) which is much lower than the
422 average values of half-saturation constants for diatoms ($1.6 \pm 1.9 \mu\text{M}$ for NO_3^- and $0.24 \pm 0.29 \mu\text{M}$
423 for PO_4^{3-} ; Sarthou et al., 2005). For Si(OH)_4 , surrounding surface concentrations at DCM ($2.39 \mu\text{M}$)
424 were in the range of diatoms half-saturation constants ($3.9 \pm 5.0 \mu\text{M}$; Sarthou et al., 2005), hence the



425 diatoms development was probably not limited by Si(OH)_4 . Furthermore, diatoms showed low
426 abundance in spite of relatively high Si(OH)_4 and dissolved trace metals (in particular Fe)
427 concentrations in surface waters. The potential of Fe limitation on phytoplankton community has
428 been reported previously in upwelling systems, with an apparent half-saturation constant for diatoms
429 growth of 0.26 nM Fe in the Peru Upwelling system (Hutchins et al., 2002). This constant is far lower
430 than the concentration of Fe measured in surrounding waters at DCM ($1.08 \pm 0.03 \mu\text{M}$ at D4),
431 suggesting that diatoms were probably not limited by Fe. This further supports growth limitation of
432 diatoms by NO_3^- and/or PO_4^{3-} .

433 Advection of waters from Amazon and Orinoco rivers can explain the relatively high Si(OH)_4
434 observed in the Caribbean Sea. However, little information is available on the input of trace metals
435 by these waters into the Caribbean Sea. Amazon river can be a source of dissolved Fe, Cu, Ni, Pb
436 and Co for the western-subtropical North Atlantic (Tovar-Sanchez and Sañudo-Wilhelmy, 2011), but
437 this input can decrease rapidly away from its source like it has been shown for Co in the Western
438 Atlantic (Dulaquais et al., 2014). Those inputs into the Caribbean Sea will have to be further
439 examined, especially for Fe, Cd, Ni, Zn, Mn whose relatively high concentrations were detected in
440 the Si(OH)_4 -enriched surface waters of this study. Additionally, other inputs of trace metals such as
441 atmospheric deposition can also increase surface concentrations, and those inputs can be substantial
442 (Shelley et al., 2012).

443 4.1.3. Primary production

444 Despite low V_c on D0 and D6 at the DCM, primary production still indicated much higher value
445 on D0 compared to D6 that was associated with higher TChl *a* (Fig. 4a). The decrease of divinyl-
446 chlorophyll *a* (*Prochlorococcus*) concentration [58] over the 6 days of observation can account for the
447 decrease of TChl *a*, whereas chlorophyll *a* concentrations did not vary significantly during this period.
448 The *Prochlorococcus* abundance was also lower by two-times on D6 compared to D0 (Fig. 6a). On
449 the contrary, fucoxanthin (diatoms) increased by four-times over the 6 days (Fig. 4 a), as well as the
450 diatoms abundance (by three-times; Fig. 5a). In turn, the increase in diatoms abundance was not
451 associated with an increase in primary production. Instead, the observed decrease in primary
452 production can be due to the decrease in *Prochlorococcus* abundance. In tropical and subtropical
453 waters, pico-phytoplankton can indeed contribute to more than 80 % of the primary production
454 (Platt et al., 1983; Goericke and Welschmeyer, 1993). The development of diatoms population likely
455 did not compensate the large decrease in *Prochlorococcus* abundance (from 141 to 63 10^3 cells mL⁻¹).
456 1).

457



458 **4.2. Impact of deep seawater discharge**

459 **4.2.1. Temperature effects**

460 The numerical simulation showed that the area impacted in the top-150 m by a temperature
461 difference larger than or equal to 0.3 °C (absolute value) was lower than 1 km² (~2-3 % of the
462 considered domain) and was insensitive to the injection depth or to the size of the tested domain
463 (Table 2). This suggests that temperature difference might rather be linked to internal variability of
464 the system. Since the effect of the discharge appears undetectable within 2-3 % variation of the
465 model, it can be deduced that in a worst-case scenario, only 3 % of the small domain (300 m along
466 the section, down to the 150 m depth) would be impacted by a temperature difference larger than
467 or equal to 0.3 °C (absolute value). The impact of a 0.3 °C temperature variation on the growth of
468 diatoms, notably on *Pseudonitzschia pseudodelicatissima* species that were observed in our study
469 area, is limited to a change in the growth rate of 0.03 d⁻¹ [61]. For *Synechococcus*, a 0.3 °C variation
470 of the temperature would also have a limited impact on the growth, with a variation of only 0.02 d⁻¹
471 (Boyd et al., 2013), like for *Emiliana huxleyi* (coccolithophyceae) for which the induced variation of
472 maximum growth rate will be lower than 0.01 d⁻¹ (Fielding, 2013). The thermal effect on the
473 phytoplankton assemblage could thus be considered negligible.

474

475 **4.2.2. Impact on the phytoplankton community**

476 Microcosms enrichment of DCM waters with 10 % of deep seawater led after 6 days to a
477 significant increase ($p < 0.05$) of fucoxanthin (diatoms) and 19'-butanoyloxyfucoxanthin
478 (haptophytes) by 71 % and 77 %, respectively, as compared to the controls. If the 2 % enrichment
479 also showed similar trends, the differences of diagnostic pigments concentrations were not
480 significant. NO₃⁻ and PO₄³⁻ concentrations induced by 10 % deep-water input on D0 ($2.57 \pm 0.13 \mu\text{M}$
481 and $0.14 \pm 0.2 \mu\text{M}$, respectively; Giraud et al., 2016) were close to NO₃⁻ and PO₄³⁻ half-saturation
482 constants of diatoms ($1.6 \pm 1.9 \mu\text{M}$ and $0.24 \pm 0.29 \mu\text{M}$, respectively; Sarthou et al., 2005). The 10 %
483 enrichment could thus support a development of diatoms. On the contrary, NO₃⁻ and PO₄³⁻
484 enrichments induced by 2 % addition of deep-water were too low ($0.57 \pm 0.02 \mu\text{M}$ and 0.04 ± 0.00
485 μM , respectively; Giraud et al., 2016) compared to these half-saturation constants to support the
486 diatoms development. Therefore, the diagnostic pigments suggested a significant response
487 proportionally to the amount of added deep seawater.

488 *Prochlorococcus* were also more abundant ($p < 0.05$) in 2 % and 10 % treatments as compared to
489 the controls. This lack of further *Prochlorococcus* population increase in 10 % treatments could be



490 attributed to a higher grazing pressure by haptophytes and/or to NO_3^- and PO_4^{3-} too rich conditions
491 (Giraud et al., 2016).

492 Phytoplankton assemblage widely evolved in surrounding waters, from a predominance of pico-
493 phytoplankton (*Prochlorococcus*) on D0 towards a higher abundance of micro-phytoplankton
494 (diatoms) on D6. In order to assess if the impact on the phytoplankton assemblage due to 10 %
495 deep seawater addition (with a shift towards the diatoms) was in the range of the natural variation
496 observed in the surrounding surface waters, 10 % deep seawater microcosms phytoplankton
497 assemblage was compared to the natural phytoplankton assemblage.

498 Whereas microcosm controls showed a lower *Prochlorococcus* abundance (Fig. 9a) than
499 surrounding surface waters on D6 ($p < 0.05$), the 10 % microcosms additionally showed, higher
500 fucoxanthin (diatoms) and 19'-butanoyloxyfucoxanthin (haptophytes) by about 142 % and 317 %
501 (Fig. 8), respectively, as compared to natural waters at D6. Furthermore, 10 % enrichments showed a
502 fucoxanthin increase over the 6 days period by 3-times higher than in surrounding waters, whereas
503 controls only showed an increase by 1.5-times higher than in surrounding waters. Therefore, it can
504 be concluded that the 10 % deep seawater enrichment induced higher variations of the
505 phytoplankton assemblage than those observed from D0 to D6 in surrounding surface waters.

506 V_c were higher ($p < 0.05$) both in 2 % and 10 % enrichments on D0 as compared to controls,
507 suggesting a positive response of phytoplankton to the deep seawater addition. Conversely, there
508 was no carbon-uptake rate difference ($p < 0.05$) between controls and enriched waters (with 2 % and
509 10 % of deep seawater) at D6 with the 6 days incubated microcosms, suggesting that the observed
510 community modifications did not change the primary production. Indeed, the phytoplankton
511 community was quite similar in surrounding surface waters on D6 and in 6 days-incubated microcosm
512 controls. Thus, only the initial phytoplankton assemblage and initial primary production in
513 surrounding surface waters would influence the response of the phytoplankton community and its
514 production.

515 At the BEL, after 6 days of incubation, deep seawater addition experiments clearly showed lower
516 effects on the phytoplankton community than at the DCM. Indeed, whereas significant differences
517 ($p < 0.05$) between 10 % enrichments and controls were observed in diagnostic pigments
518 concentrations at the DCM, pigments concentrations were too low at the BEL to be quantified. It
519 can be suggested that the lower population and lower carbon uptake could be related to the lowest
520 light availability.

521 Overall, the phytoplankton response was proportional to the amount of added deep seawater. If
522 the phytoplankton assemblage significantly varied over time in the environment, the 10 % deep
523 seawater enrichment showed larger variations (for diatoms and haptophytes) than those observed in



524 the natural environment. The DCM should be more impacted than the BEL by the deep seawater
525 discharge even with a large deep seawater input. On the other hand, the impact on the primary
526 production largely depended on the initial phytoplankton assemblage, which was quite variable over
527 time. The modification of the phytoplankton community to a deep seawater input could also be
528 depending on the initial phytoplankton community. For that, the microcosm experiments did not
529 allow drawing a scenario over the long term of the potential modifications of the primary production
530 and the phytoplankton community associated to the deep seawater discharge by an OTEC.

531 Light microscopy analyses showed a large abundance of dinoflagellates at the DCM (between
532 9,240 and 20,400 cells mL⁻¹ on D6 and D4; Fig. 5 a) which could be mixotrophic or heterotrophic and
533 thus probably exert a grazing pressure on the phytoplankton, particularly on the pico-phytoplankton
534 (Liu et al., 2002). However, in this study, the zooplankton larger than 200 µm and its potential control
535 on the phytoplankton community were not considered and should be examined in future studies.

536 5. Conclusion

537 Two complementary approaches were applied to study the potential effects of the deep
538 seawater discharge of the planned OTEC plant on the phytoplankton community off Martinique.

539 Because the distribution and the development of phytoplankton are directly linked to the surface
540 stratification, it is important to assess the thermal effect of deep seawater by an OTEC plant.
541 Modelling of the deep seawater discharge showed that the thermal structure of the top 150 m of the
542 water column on large and near-OTEC sections should be very slightly impacted for the lowest
543 considered temperature differences $|\Delta T| \geq 0.3$ °C. If World Bank Group prescriptions of not
544 exceeding a higher temperature difference of 3 °C are followed, the environmental perturbations
545 potentially caused by the operation of the OTEC should be considered negligible. The area where
546 the 150 m-depth waters are impacted by the lowest considered temperature differences $|\Delta T| \geq 0.3$
547 °C would not exceed 1 km² in a worst-case scenario.

548 The phytoplankton community and its production could be impacted by a large deep seawater
549 input. Whereas pico-phytoplankton currently largely dominates the phytoplankton assemblage, a
550 ratio of 10 % of deep seawater in DCM waters could induce a shift toward the diatoms and micro-
551 phytoplankton. The ratio of 2 % of deep seawater in DCM waters only showed significant higher
552 *Prochlorococcus* abundance than controls, but the assemblage and the primary production were not
553 modified by this lower input. The stimulation of *Prochlorococcus* could be due to one or some of the
554 following causes: NO₃⁻ and/or PO₄³⁻ supply, trace metal supply, lowered pH (higher availability of
555 dissolved inorganic carbon).



556 Although significant, these results would have to be extended to larger temporal scale, and the
557 phytoplankton interactions with higher trophic levels (such as zooplankton) must be studied.
558 Because no environment standards on the deep seawater discharge effects are available yet, a
559 rigorous monitoring of the phytoplankton community, biogeochemical parameters distribution and
560 of the water column stratification must be established as soon as the OTEC is implemented and
561 during its continuous functioning.

562 **Acknowledgements**

563 This work was supported by France Energies Marines and part of the IMPALA project. We would like
564 to thank the Captains and crew members of the “Pointe d’Enfer”, and the scientists in the laboratory
565 at the University of the French West Indies and Guiana at Martinique; Dominique Marie (UPMC,
566 Roscoff, France) and Christophe Lambert (LEMAR, France) for their help with the flow cytometry,
567 and Anne Donval (LEMAR, France) for the pigment analyses.

568

569



570 **References**

571 Agawin, N.S.R., Duarte, C.M., Agustí, S.: Nutrient and temperature control of the contribution
572 of picoplankton to phytoplankton biomass and production. *Limnology and Oceanography*,
573 45(8), 1891–1891, 2000.

574 Aminot, A., and Kérouel, R.: Dosage automatique des nutriments dans les eaux marines : méthodes
575 en flux continu. Ifremer Eds., *Méthodes d'analyse en milieu marin*, Quae, 2007.

576 Aure, J., Strand, O., Erga, S.R., Strohmeier, T.: Primary production enhancement by artificial
577 upwelling in a western Norwegian fjord, *Marine Ecology Progress Series*, 39–470 52, 2007.

578 Bakun, A.: Global climate change and intensification of coastal ocean upwelling, *Science*, 247(4939),
579 198–201, 1990.

580 Boyd, P. W., Jickells, T., Law, C. S., Blain, S., Boyle, E. A., Buesseler, K. O., et al.: Mesoscale iron
581 enrichment experiments 1993-2005: Synthesis and future directions, *Science*, 315(5812), 612–617,
582 2007.

583 Boyd, P.W., Rynearson, T.A., Armstrong, E.A., Fu, F., Hayashi, K., Hu, Z. et al.: Marine phytoplankton
584 temperature versus growth responses from polar to tropical waters—outcome of a scientific
585 community-wide study, *PLoS One*, 8(5), e63091, 2013.

586 Bruland, K. W., Rue, E. L., Smith, G. J.: Iron and macronutrients in California coastal upwelling
587 regimes: Implications for diatom blooms, *Limnology and Oceanography*, 46, 1661–1674, 2001.

588 Bruland, K.W.: Controls on trace metals in seawater, *The Oceans and Marine Geochemistry*,
589 *Treatise on Geochemistry*, 6, 23–47, 2003.

590 Brzezinski, M.A.: The Si:C:N ratio of marine diatoms. Interspecific variability and the effect of
591 environmental variables, *Journal of Phycology*, 21, 347–357, 1985.

592 Carr, M. E., and Kearns, E. J.: Production regimes in four Eastern Boundary Current systems, *Deep
593 Sea Research Part II: Topical Studies in Oceanography*, 50(22), 3199–3221, 2003.

594 Carton, J.A., and Giese, B.S.: A reanalysis of ocean climate using Simple Ocean Data Assimilation
595 (SODA), *Monthly Weather Review*, 136(8), 2999–3017, 2008.



- 596 Casey, J. R., Lomas, M.W., Mandecki, J., Walker, D.E.: Prochlorococcus contributes to new
597 production in the Sargasso Sea deep chlorophyll maximum. *Geophysical Research Letters*, 34(10),
598 2007.
- 599 Chavez, F.P., Toggweiler, J.R.: Physical estimates of global new production: the upwelling
600 contribution. In: Summerhayes, C.P., Emeis, K.C., Angel, M.V., Smith, R.L., Zeitzschel, B. (Eds.),
601 *Upwelling in the Ocean: Modern Processes and Ancient Records*. Wiley, 313–320, 1995.
- 602 De Baar, H. J., Boyd, P. W., Coale, K. H., Landry, M. R., Tsuda, A., et al.: Synthesis of iron fertilization
603 experiments: from the Iron Age in the age of enlightenment, *Journal of Geophysical Research:*
604 *Oceans* (1978–2012), 110(C9), 2005.
- 605 Duarte, C.M., Agusti, S., Agawin, N.S.R.: Response of a Mediterranean phytoplankton community to
606 increased nutrient inputs: a mesocosm experiment, *Marine Ecology Progress Series*, 195, 61–70,
607 2000.
- 608 Dugdale, R.C., and Wilkerson, F.P.: The use of ^{15}N to measure nitrogen uptake in eutrophic oceans;
609 experimental considerations, *Limnology and Oceanography*, 31(4), 673–689, 1986.
- 610 Dulaquais, G., Boye, M., Rijkenberg, M.J.A., Carton, X.J.: Physical and remineralization processes
611 govern the cobalt distribution in the deep western Atlantic Ocean. *Biogeosciences*, 11(6), 1561–
612 1580, 2014.
- 613 Dussart, B.M.: Les différentes catégories de plancton, *Hydrobiologia*, 26, 72–74, 1966.
- 614 Edmond, J. M., Boyle, E. A., Grant, B., Stallard, R.F.: The chemical mass balance in the Amazon
615 plume I: The nutrients, *Deep Sea Research Part A. Oceanographic Research Papers*, 28(11), 1339–
616 1374, 1981.
- 617 Escaravage, V., Prins, T.C., Smaal, A.C., Peeters, J.C.H.: The response of phytoplankton communities
618 to phosphorus input reduction in mesocosm experiments, *Journal of Experimental Marine Biology*
619 *and Ecology*, 198, 55–79, 1996.
- 620 Fernández, I., Raimbault, P., Garcia, N., Rimmelin, P., Caniaux, G.: An estimation of annual new
621 production and carbon fluxes in the northeast Atlantic Ocean during 2001, *Journal of Geophysical*
622 *Research: Oceans* (1978–2012), 110(C7), C07S13, 2005.



- 623 Fielding, S.R.: *Emiliania huxleyi* specific growth rate dependence on temperature, *Limnol. &*
624 *Oceanogr*, 58(2), 663–666, 2013.
- 625 Giraud, M., Boye, M., Garçon, V., Donval, A., De La Broise, D.: Simulation of an artificial upwelling
626 using immersed in situ phytoplankton microcosms, *Journal of Experimental Marine Biology and*
627 *Ecology*, 475, 80–88, 2016.
- 628 Goericke, R. and Welschmeyer, N.A.: The Marine Prochlorophyte *Prochlorococcus* Contributes
629 Significantly to Phytoplankton Biomass and Primary Production in the Sargasso Sea, *Deep Sea*
630 *Research Part I: Oceanographic Research Papers*, 40(11), 2283-2294, 1993.
- 631 Goericke, R., and Repeta, D.J.: The pigments of *Prochlorococcus marinus*: The presence of divinyl
632 chlorophyll a and b in a marine prochlorophyte. *Limnology and Oceanography*, 37, 425–433, 1992.
- 633 Gruber, N.: The marine nitrogen cycle: overview and challenges, *Nitrogen in the marine*
634 *environment*, 1–50, 2008.
- 635 Handå, A., McClimans, T.A., Reitan, K.I., Knutsen, Ø., Tangen, K., Olsen, Y.: Artificial upwelling to
636 stimulate growth of non-toxic algae in a habitat for mussel farming, *Aquaculture Research*, 45, 1798–
637 1809, 2014.
- 638 Harrison, W.G., Harris, L.R., Irwin, B.D.: The kinetics of nitrogen utilization in the oceanic mixed layer:
639 Nitrate and ammonium interactions at nanomolar concentrations, *Limnology and Oceanography*,
640 41(1), 16–32, 1996.
- 641 Hasle, G.R.: The inverted microscope method, In: Sournia, A. (Ed.), *Phytoplankton Manual*. UNESCO,
642 Paris, 1988.
- 643 Hillebrand, H., Durselen, C.D., Kirchtel, D., Pollinger, U., Zohary, T.: Biovolume calculation for
644 pelagic and benthic microalgae, *Journal of Phycology*, 35, 403–424, 1999.
- 645 Hooker, S.B., Clementson, L., Thomas, C.S., Schlüter, L., Allerup, M., Ras, J., Claustre, H., et al.:
646 NASA Tech. Memo. 2012-217503, NASA Goddard Space Flight Center, Greenbelt, Maryland,
647 2012.
- 648 Hu, C., Montgomery, E.T., Schmitt, R.W., Muller-Karger, F.E.: The dispersal of the Amazon and
649 Orinoco River water in the tropical Atlantic and Caribbean Sea: Observation from space and S-



- 650 PALACE floats, *Deep Sea Research Part II: Topical Studies in Oceanography*, 51(10–11), 1151–1171,
651 2004.
- 652 Hutchins, D.A., Hare, C.E., Weaver, R.S., Zhang, Y., Firme, G.F., DiTullio, G.R., Alm, M.B.,
653 Riseman, S.F., Maucher, J.M., Geesey, M.E., Trick, C.G., Smith, G.J., Rue, E.L., Conn, J.,
654 Bruland, K.W.: Phytoplankton iron limitation in the Humboldt current and Peru upwelling,
655 *Limnology and Oceanography*, 47, 997–1011, 2002.
- 656 International Finance Corporation (IFC): World Bank Group, Environmental, Health, and Safety
657 Guidelines for Liquefied Natural Gas (LNG) Facilities, 2007.
- 658 Kagaya, S., Maeba, E., Inoue, Y., Kamichatani, W., et al.: A solid phase extraction using a chelate
659 resin immobilizing carboxymethylated pentaethylenhexamine for separation and preconcentration
660 of trace elements in water samples, *Talanta*, 79(2), 146–152, 2009.
- 661 Kress, N., Thingstad, T.F., Pitta, P., Psarra, S., Tanaka, T., Zohary, T., Groom, S., Herut, B., Mantoura,
662 R.F.C., Polychronaki, T., Rassoulzadegan, F., Spyres G.: Effect of P and N addition to oligotrophic
663 Eastern Mediterranean waters influenced by near-shore waters: a microcosm experiment, *Deep Sea
664 Research Part II: Topical Studies in Oceanography*, 52, 3054–3073, 2005.
- 665 Liu, H., Suzuki, K., Saino, T.: Phytoplankton growth and microzooplankton grazing in the subarctic
666 Pacific Ocean and the Bering Sea during summer 1999, *Deep Sea Research Part I: Oceanographic
667 Research Papers*, 49(2), 363–375, 2002.
- 668 Lundholm, N., Skov, J., Pocklington, R., Moestrup, Ø.: Studies on the marine planktonic diatom
669 *Pseudo-nitzschia*. 2. Autecology of *P. pseudodelicatissima* based on isolates from Danish coastal
670 waters, *Phycologia*, 36(5), 381–388, 1997.
- 671 Marie, D., Partensky, F., Vaulot, D., Brussaard, C.: Enumeration of phytoplankton, bacteria, and
672 viruses in marine samples, *Current protocols in cytometry*, 1–11, 1999.
- 673 Mawji, E., Schlitzer, R., et al.: The GEOTRACES intermediate data product 2014, *Marine
674 Chemistry*, 177(1), 1–8, 2015, doi 10.1016/j.marchem.2015.04.005.
- 675 Milne, A., Landing, W., Bizimis, M., Morton, P.: Determination of Mn, Fe, Co, Ni, Cu, Zn, Cd and Pb
676 in seawater using high resolution magnetic sector inductively coupled mass spectrometry (HR-ICP-
677 MS). *Analytica Chimica Acta*, 665(2), 200–207, 2010.



- 678 Moore, W.S., Sarmiento, J.L.R., Key, M.: Tracing the Amazon component of surface Atlantic water
679 using ^{228}Ra , salinity and silica, *Journal of Geophysical Research: Oceans* (1978–2012), 91(C2), 2574–
680 2580, 1986.
- 681 Muller-Karger, F.E., McClain, C.R., Richardson, P.L.: The dispersal of the Amazon's water. *Nature*,
682 333, 56–58, 1988.
- 683 Muller-Karger, F.E., Richardson, P.L., McGillicuddy, D.: On the offshore dispersal of the Amazon's
684 plume in the North Atlantic, *Deep-Sea Research*, 42, 2127–2137, 1995.
- 685 National Oceanic and Atmospheric Administration (NOAA): Ocean thermal energy conversion final
686 environmental impact statement. Office of Ocean Minerals and Energy, Charleston, SC, 1981.
- 687 National Oceanic and Atmospheric Administration (NOAA): Ocean thermal energy conversion:
688 Assessing potential physical, chemical, and biological impacts and risks. University of New
689 Hampshire, Durham, NH, 2010.
- 690 Nozaki, Y.: A fresh look at element distribution in the North Pacific Ocean, *Eos Transaction*, 78(21),
691 221, 1997.
- 692 Orr, J.C., et al.: Anthropogenic ocean acidification over the twenty-first century and its impact
693 on calcifying organisms, *Nature*, 437(7059), 681–686, 2005.
- 694 Osborne, A.H., Haley, B.A., Hathorne, E. C., Flögel, S., Frank, M.: Neodymium isotopes and
695 concentrations in Caribbean seawater: Tracing water mass mixing and continental input in a semi-
696 enclosed ocean basin, *Earth and Planetary Science Letters*, 406, 174–186, 2014.
- 697 Osborne, A.H., Haley, B.A., Hathorne, E. C., Plancherel, Y., Frank, M.: Rare earth element
698 distribution in Caribbean seawater: Continental inputs versus lateral transport of distinct REE
699 compositions in subsurface water masses, *Marine Chemistry*, 177, 172–183, 2015.
- 700 Partensky, F., Hess, W.R., Vaulot, D.: *Prochlorococcus*, a marine photosynthetic prokaryote of global
701 significance, *Microbiology and Molecular Biology Reviews*, 63 (1), 106–127, 1999.
- 702 Pauly, D., and Christensen, V.: Primary production required to sustain global fisheries, *Nature*,
703 374(6519), 255–257, 1995.



- 704 Platt, T., Rao, D. S., Irwin, B.: Photosynthesis of picoplankton in the oligotrophic ocean, *Nature*, 301,
705 702–704, 1983.
- 706 Rocheleau, G., Hamrick, J., Church, M.: Modeling the Physical and Biochemical Influence of Ocean
707 Thermal Energy Conversion Plant Discharges into their Adjacent Waters, Final Technical Report, U.S.
708 Department of Energy Award N° DE-EE0003638, Makai Ocean Engineering, Inc., Kailua, Hawaii,
709 2012.
- 710 Sarthou, G., Timmermans, K.R., Blain, S., Tréguer, P.: Growth physiology and fate of diatoms in the
711 ocean: a review, *Journal of Sea Research*, 53(1), 25–42, 2005.
- 712 Shchepetkin, A.F., and McWilliams, J.C.: Correction and commentary for “Ocean forecasting in
713 terrain-following coordinates: Formulation and skill assessment of the regional ocean modeling
714 system” by Haidvogel et al., *J. Comp. Phys.*, 227, 3595–3624, *Journal of Computational Physics*,
715 228(24), 8985–9000, 2009.
- 716 Shchepetkin, A.F., and McWilliams, J.C.: The regional oceanic modeling system (ROMS): a split-
717 explicit, free-surface, topography-following-coordinate oceanic model, *Ocean Modelling*, 9(4), 347–
718 404, 2005.
- 719 Shelley, R. U., et al.: Controls on dissolved cobalt in surface waters of the Sargasso Sea: Comparisons
720 with iron and aluminum, *Global Biogeochem. Cycles*, 26(2), GB2020, doi:10.1029/2011GB004155,
721 2012.
- 722 Slawyk, G., Collos, Y., Auclair, J.C.: The use of the ¹³C and ¹⁵N isotopes for the simultaneous
723 measurement of carbon and nitrogen turnover rates in marine phytoplankton, *Limnology and*
724 *Oceanography*, 22, 925–932, 1977.
- 725 Steven, D.M., and Brooks, A.L.: Identification of Amazon River water at Barbados, W. Indies by
726 salinity and silicate measurements. *Marine Biology*, 14, 345–348, 1972.
- 727 Taguchi, S., Jones, D., Hirata, J.A., Laws, E.A.: Potential effect of ocean thermal energy
728 conversion (OTEC) mixed water on natural phytoplankton assemblages in Hawaiian waters.
729 *Bulletin of Plankton Society of Japan*, 34(2), 125–142, 1987.



730 Tovar-Sanchez, A., and Sañudo-Wilhelmy, S.A.: Influence of the Amazon River on dissolved and intra-
731 cellular metal concentrations in *Trichodesmium* colonies along the western boundary of the sub-
732 tropical North Atlantic Ocean, *Biogeosciences*, 8, 217–225, 2011.

733 Uitz, J., Claustre, H., Gentili, B., Stramski, D.: Phytoplankton class-specific primary production in the
734 world's oceans: seasonal and interannual variability from satellite observations, *Global*
735 *Biogeochemical Cycles*, 24(3), 2010.

736 Van Oostende, N., Dunne, J. P., Fawcett, S. E., Ward, B. B.: Phytoplankton succession explains size-
737 partitioning of new production following upwelling-induced blooms, *Journal of Marine Systems*, 148,
738 14–25, 2015.

739

740 **Tables**

741

742 **Table 1-** Comparison of analyses of SAFe (Sampling and Analysis of iron) S and D2 reference
 743 samples (<http://www.geotraces.org/science/intercalibration>) between ID-ICPMS values (this study)
 744 and the consensus values. Our mean reagent blanks (based on all blank determinations) for dissolved
 745 Cd, Pb, Fe, Ni, Cu, Zn, Mn and Co, and detection limits of ID-ICPMS estimated as three times the
 746 standard deviation of the mean reagent blanks are also shown.

747

	Cd (pM)	Pb (pM)	Fe (nM)	Ni (nM)	Cu (nM)	Zn (nM)	Mn (nM)	Co (pM)
SAFe D2								
This study	948.83 ± 65.95	28.86 ± 4.44	0.898 ± 0.098	8.60 ± 0.36	2.15 ± 0.16	7.29 ± 0.27	0.40 ± 0.05	40.12 ± 3.88
Consensus values	986.00 ± 23.00	27.70 ± 1.50	0.933 ± 0.023	8.63 ± 0.25	2.28 ± 0.15	7.43 ± 0.25	0.35 ± 0.05	45.70 ± 2.90
n=	20	20	18	19	22	13	23	23
SAFe S								
This study	7.24 ± 1.57	48.42 ± 6.08	0.087 ± 0.025	2.56 ± 0.55	0.55 ± 0.06	0.07 ± 0.06	0.75 ± 0.05	2.85 ± 0.81
Consensus values	1.10 ± 0.30	48.00 ± 2.20	0.093 ± 0.008	2.28 ± 0.09	0.52 ± 0.05	0.07 ± 0.01	0.79 ± 0.06	4.80 ± 1.20
n=	25	27	15	25	30	10	27	28
Detection Limit	0.996	0.613	0.032	0.096	0.011	0.129	0.001	0.07
Blanks	0.716	1.809	0.061	0.040	0.019	0.129	0.003	0.32

748

749

750 **Table 2-** Area (km²) impacted in the top-150 m by a temperature difference $|\Delta T| \geq 0.3$ °C on two
 751 vertical sections centered on the OTEC, considering eight depths of deep seawater discharge (45,
 752 80, 110, 140, 170, 250, 350, 500 m), average and root mean square for the year 2000 (from the
 753 monthly data) and for June 2000.

754

Depth of deep water discharge	Mean Year 2000		June 2000	
	Large domain	Near-OTEC domain	Large domain	Near-OTEC domain
45 m	0.4 ± 0.4	0.0 ± 0.1	0.0	0.0
80 m	0.6 ± 0.7	0.1 ± 0.1	0.4	0.0
110 m	0.6 ± 0.5	0.0 ± 0.1	0.9	0.0
140 m	0.4 ± 0.5	0.1 ± 0.1	0.1	0.0
170 m	0.5 ± 0.8	0.0 ± 0.1	0.5	0.0
250 m	0.5 ± 0.7	0.1 ± 0.1	0.1	0.0
350 m	0.5 ± 0.5	0.1 ± 0.1	0.0	0.0
500 m	0.5 ± 0.5	0.1 ± 0.1	0.3	0.0

755

756

757

758

759

760

761

762

763

764

765

766

767



768 **Table 3-** Nitrate, silicate, phosphate and nitrite concentrations on June 16th 2014 (D4) at the deep
 769 chlorophyll maximum (DCM), at the bottom of the euphotic layer (BEL), and at the deep seawater
 770 pumping depth. Concentrations were measured at the OTEC site (0 % addition of deep waters) and
 771 calculated for 2 % and 10 % deep seawater additions.

772

Depth (m)	Deep seawater ratio	[NO ₃ ⁻] (μM)	[Si(OH) ₄] (μM)	[PO ₄ ³⁻] (μM)	[NO ₂ ⁻] (μM)
DCM	0 %	< 0.02	2.39	< 0.02	0.02
	2 %	0.54	2.88	0.04	0.02
	10 %	2.71	4.82	0.19	0.02
BEL	0 %	< 0.02	1.46	< 0.02	0.32
	2 %	0.54	1.96	0.04	0.32
	10 %	2.71	3.98	0.19	0.29
1100	100 %	27.11	26.69	1.87	<0.02

773

774

775 **Table 4-** Concentrations of dissolved trace metals (in nM): Mn, Fe, Cd, Zn, Co, Ni, Cu, Pb measured
 776 on June 16th 2014 (D4) at the OTEC site at the DCM, BEL and 1100 m (0 % addition of deep waters),
 777 and their calculated concentrations in the mixtures with 2 % and 10 % addition of deep water.

778

Depth (m)	Deep seawater ratio	Mn (nM)	Fe (nM)	Cd (nM)	Zn (nM)	Co (nM)	Ni (nM)	Cu (nM)	Pb (nM)
DCM	0 %	2.97 ± 0.17	1.08 ± 0.03	0.03 ± 0.01	1.54 ± 0.04	0.05 ± 0.00	2.22 ± 0.10	1.70 ± 0.18	0.03 ± 0.00
	2 %	2.92	1.08	0.04	1.56	0.05	2.29	1.70	0.03
	10 %	2.71	1.09	0.07	1.63	0.05	2.60	1.71	0.03
BEL	0 %	1.65 ± 0.04	0.68 ± 0.03	0.03 ± 0.00	0.65 ± 0.03	0.03 ± 0.00	2.26 ± 0.17	1.14 ± 0.10	0.03 ± 0.00
	2 %	1.63	0.69	0.04	0.68	0.03	2.34	1.15	0.03
	10 %	1.52	0.73	0.08	0.82	0.03	2.64	1.21	0.03
1100	100 %	0.34 ± 0.02	1.22 ± 0.05	0.45 ± 0.01	2.39 ± 0.07	0.06 ± 0.00	6.00 ± 0.13	1.80 ± 0.08	0.02 ± 0.00

779

780

781 **Table 5-** Definition of the diagnostic pigments used as phytoplankton biomarkers (taxonomic
 782 significance) and associated phytoplankton size class (Uitz et al., 2010).

783

Diagnostic Pigments	Abbreviations	Taxonomic Significance	Phytoplankton Size Class
Fucoxanthin	Fuco	Diatoms	microplankton
Peridinin	Perid	Dinoflagellates	microplankton
19'-hexanoyloxyfucoxanthin	Hex-fuco	Haptophytes	nanoplankton
19'-butanoyloxyfucoxanthin	But-fuco	Pelagophytes and Haptophytes	nanoplankton
Alloxanthin	Allo	Cryptophytes	nanoplankton
chlorophyll <i>b</i> + divinyl chlorophyll <i>b</i>	TChlb	Cyanobacteria, Prochlorophytes	picoplankton
Zeaxanthin	Zea	Chlorophytes, Prochlorophytes	picoplankton

784

785



786

787 **Figure captions**

788

789 **Figure 1-** Bathymetry of the parent and child (grey rectangle) domains interpolated from the GINA
790 data base with a zoom on the near domain (black rectangle); the oblique white and black lines
791 represent the large and small sections, respectively, used for numerical simulations.

792

793 **Figure 2-** Comparison of temperature and salinity between model outputs and field data at the
794 OTEC station (a) on June 16th 2000 and 2014, respectively and (b) on November 28th 2000 and 2013,
795 respectively.

796

797 **Figure 3-** Comparison of mean current direction and horizontal velocity norm between model
798 outputs from June 2000 and ADCP data from June 2011.

799

800 **Figure 4-** Pigment concentrations (from HPLC analysis) at the OTEC site at the DCM (a) and at the
801 BEL (b), on June 12th (D0), 16th (D4), 18th (D6) 2014 (bars represent the standard deviation).

802

803 **Figure 5-** Abundance and biovolume of micro- and part of nano-phytoplankton at the OTEC site on
804 June 12th (D0), 16th (D4), 18th (D6) 2014, at the DCM (a and c, respectively) and at the BEL (b and d,
805 respectively) (bars represent the standard deviation).

806

807 **Figure 6-** Abundance of pico-phytoplankton at the DCM (a) and at the BEL (b), on June 12th (D0),
808 16th (D4), 18th (D6) 2014 (bars represent the standard deviation).

809

810 **Figure 7-** Specific carbon uptake rate (h^{-1}) at the DCM (a) and BEL (b) depths, on June 12th (D0), and
811 18th (D6), and in 6 days incubated microcosms (D6), for the three mixing conditions (0 %, 2 % and 10
812 % of deep seawater additions) (for surrounding waters bars represent the standard deviation for 3
813 replicates).

814

815 **Figure 8-** Diagnostic pigment concentrations in surrounding surface waters on D0 and D6, and in
816 controls and deep water-enriched (2 % and 10 %) microcosms after 6 days of incubation at the DCM
817 (bars represent the standard deviation). Similar letters (a, b or c) attributed to 2 or more treatments
818 indicate no significant differences ($p < 0.05$) between these treatments.

819

820 **Figure 9-** Abundance of picophytoplankton in surrounding surface waters on day 0 and 6, and in
821 controls and deep water-enriched (2 % and 10 %) microcosms after 6 days of incubation at 45 m
822 depth (a) and 80 m depth (b) (bars represent the standard deviation). Similar letters (a, b or c)
823 attributed to 2 or more treatments indicate no significant differences ($p < 0.05$) between these
824 treatments.

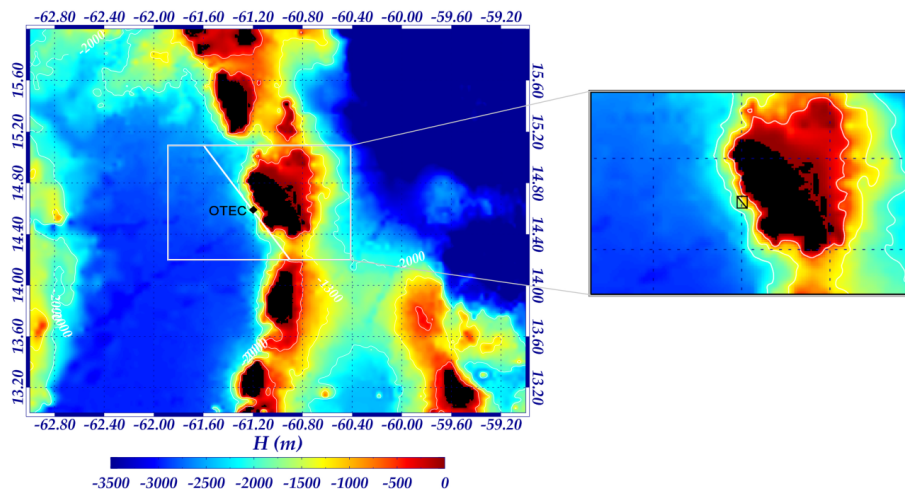
825



826

827 **Figure 1**

828



829

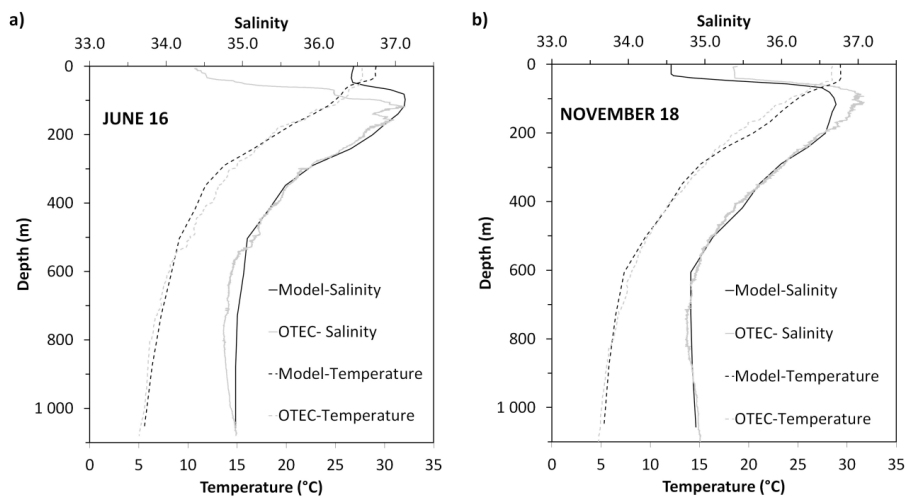
830

831

832

833 **Figure 2**

834



835

836

837

838

839

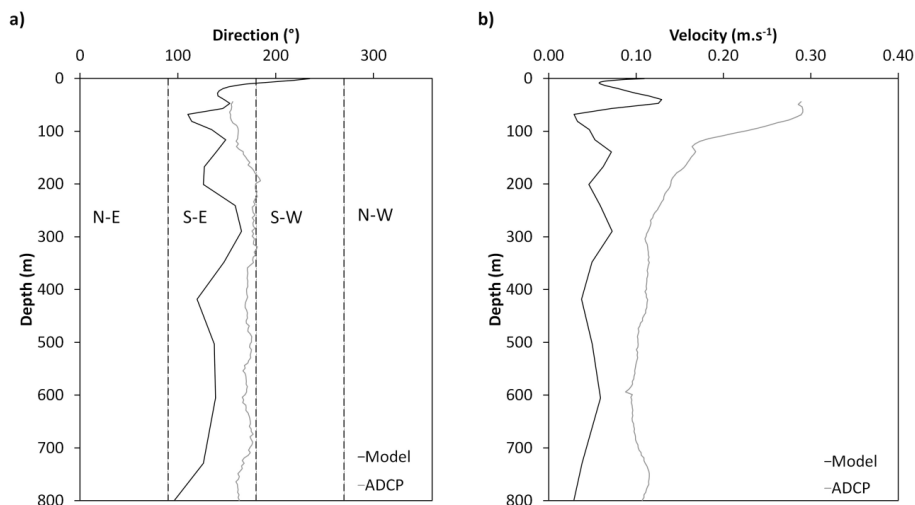
840

841



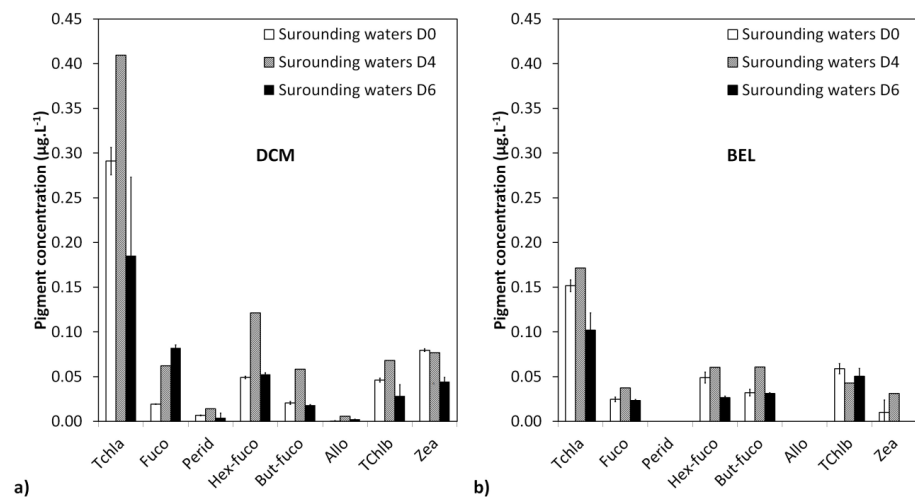
842
 843
 844
 845
 846
 847
 848

Figure 3



849
 850
 851
 852
 853
 854
 855

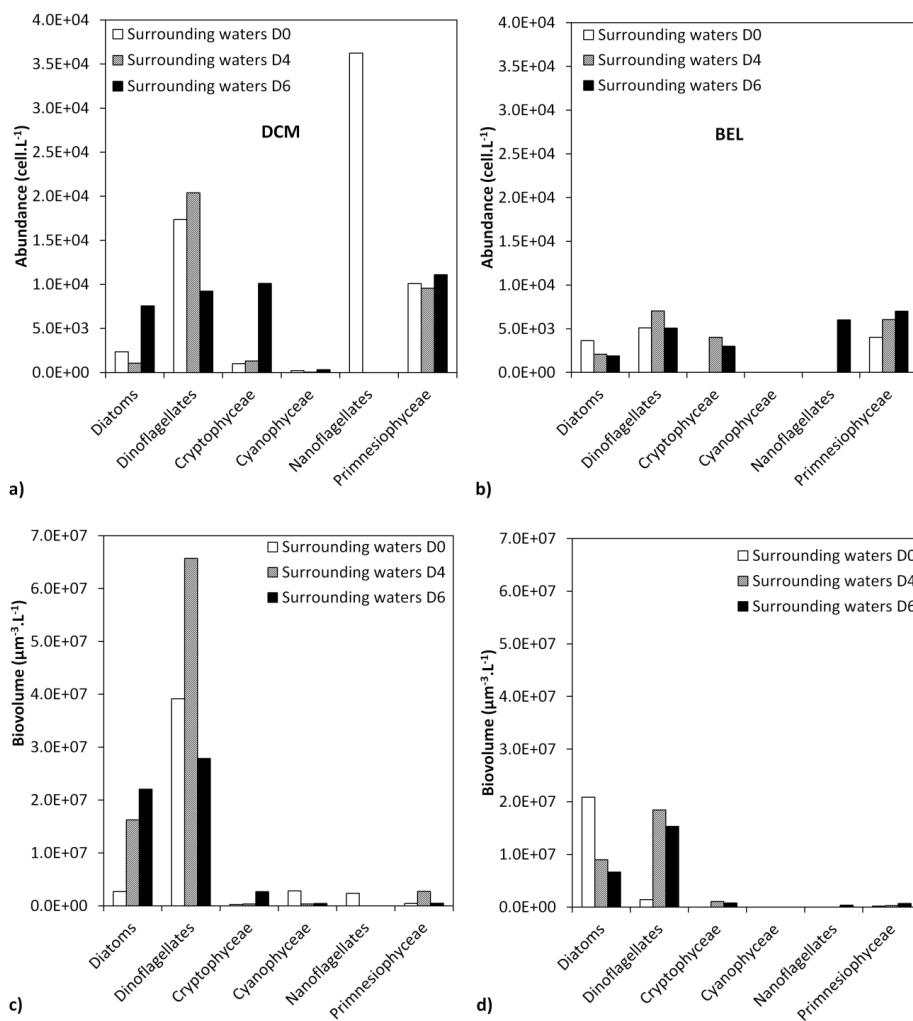
Figure 4



856
 857
 858
 859



860 **Figure 5**

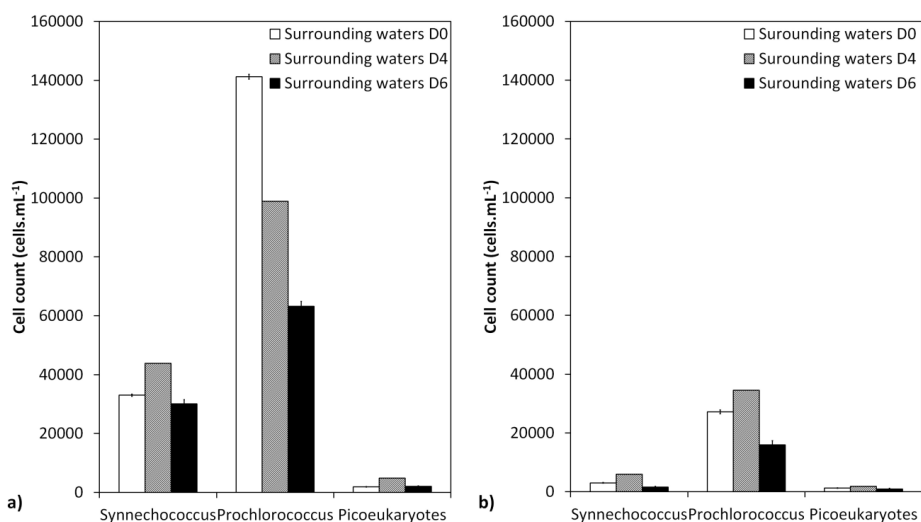


861
 862
 863
 864
 865
 866
 867
 868
 869
 870
 871
 872
 873
 874



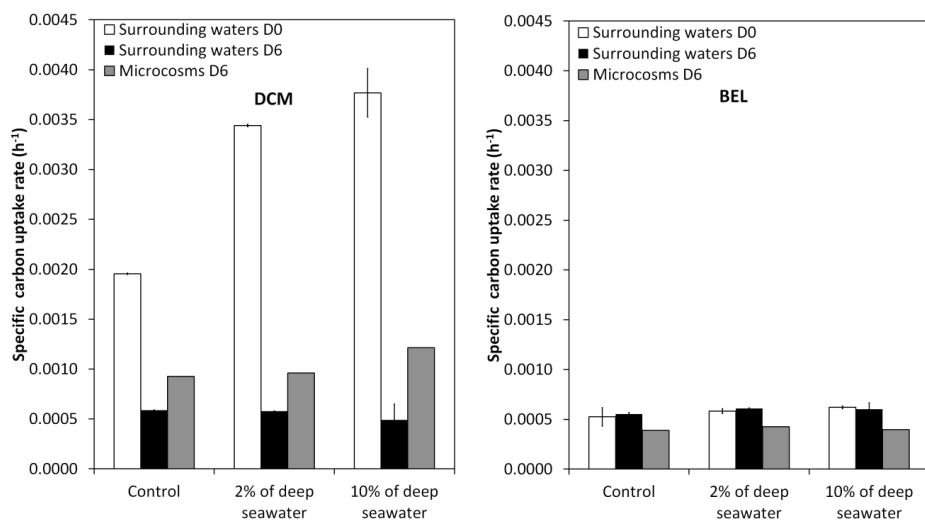
875
 876
 877
 878
 879

Figure 6



880
 881
 882
 883
 884

Figure 7

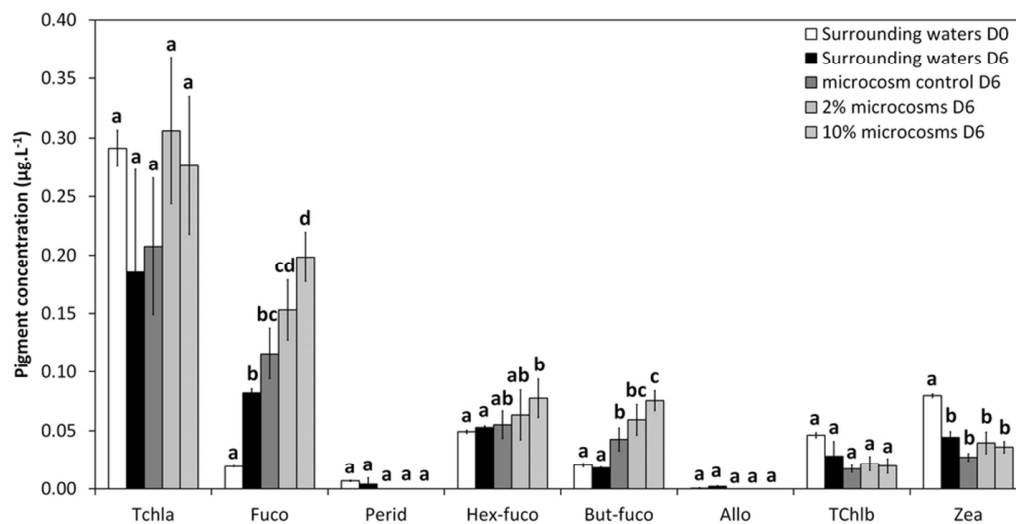


885
 886
 887
 888
 889
 890
 891



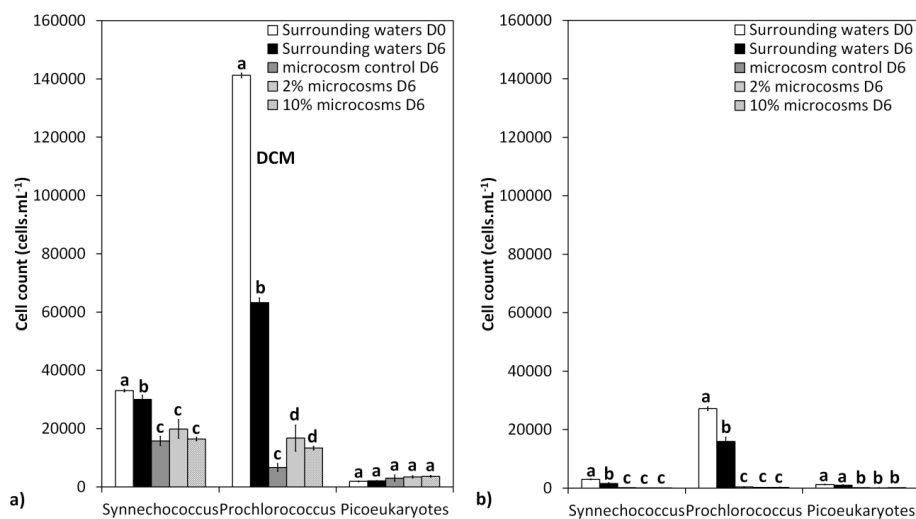
892
 893
 894
 895

Figure 8



896
 897
 898
 899
 900

Figure 9



901
 902
 903